Astron. Astrophys. 325, 709–713 (1997)

ASTRONOMY AND ASTROPHYSICS

Chromospheric velocity fields in α Orionis (M2 Iab) generated by stochastic shocks

M. Cuntz[1,2]

[1] Center for Space Plasma and Aeronomic Research (CSPAR), EB 136M, University of Alabama in Huntsville, Huntsville, AL 35899, USA
[2] Institut für Theoretische Astrophysik der Universität Heidelberg, Tiergartenstr. 15, D-69121 Heidelberg, Germany

Received 24 February 1997 / Accepted 25 March 1997

Abstract. I present results from recent ab-initio models for the formation and time-dependent behavior of outer atmospheric flows in α Ori (M2 Iab) produced by stochastic shock waves. Stochastic shocks are a natural consequence of acoustic energy generation due to stellar convection. The wave models show distinct episodes of momentum and energy deposition produced by strong shocks generated by merging of shocks in the stochastic wave field. It is found that sub- and supersonic inflows and outflows are generated at different atmospheric heights as function of the wave parameters adopted. The flow velocities given by the models encompass the velocity range revealed by the Fe II emission line components given by recent GHRS data (Carpenter & Robinson 1997). This result is evidence that nonmagnetic wave modes are relevant for the heating and dynamics of the outer atmosphere of α Ori and possibly other M-type supergiants as well, although it does not preclude the possibility that magnetic heating may be equally or more important.

Key words: hydrodynamics – shock waves – waves – stars: chromospheres – stars: individual: α Ori – stars: supergiants

1. Introduction

The M-type supergiant α Ori (M2 Iab) is a well studied object and a broad range of dynamical atmospheric features has been identified. Alpha Ori is a noncoronal star with an extended atmosphere and a cool, massive wind. Alpha Ori has an extended chromosphere with temperatures in excess of 6000 K (Newell & Hjellming 1982). The size of the chromosphere is uncertain as it is probably strongly dependent on the spectral diagnostics used. Basri et al. (1981) have calculated a semiempirical chromosphere model for α Ori by fitting the Mg II and Ca II line fluxes given by IUE assuming smooth functions for the atmospheric density and pressure. They found a steady increase of the atmospheric temperature starting from 2820 K in the temperature minimum layer up to 7000 K at a mass column density of $1 \cdot 10^{-6}$ g cm^{-2}. These observational data have been re-interpreted by Hartmann & Avrett (1984) assuming a combined chromosphere-wind model. The model was calculated considering momentum deposition by Alfvén waves described by means of a time-independent dissipation law. Theoretical calculations based on stochastic acoustic shocks have been given by Cuntz (1992a,b). These models are self-consistent, time-dependent and fully nonlinear. They give information about the propagation and dissipation of nonmagnetic energy in the chromosphere and allow predictions about the expected range of chromospheric temperatures and velocity fields.

In the meantime, high resolution spectra obtained by HST-GHRS have become available. Results are given by Carpenter et al. (1994a,b), Robinson & Carpenter (1995), Brandt et al. (1995), and Carpenter & Robinson (1997). These data contain a large amount of novel spectral information, largely because of the increase in spectral resolution. They also indicate the presence of complex chromospheric velocity fields (both sub- and supersonic, both inwardly and outwardly directed flows), which *in principle* cannot be explained by either the semiempirical model of Basri et al. (1981) or the time-independent Alfvén wave driven wind model given by Hartmann & Avrett (1984). The various components of the Fe II emission features, for instance, point to the existence of different dynamic atmospheric components with radial velocities ranging from -14 km s^{-1} (inwardly directed) to +15 km s^{-1} (outwardly directed) relative to the stellar photosphere (Carpenter & Robinson 1997). A further interesting velocity feature was described by Robinson & Carpenter (1995). They found that the Mg II lines, which have profiles similar to the strong Fe II lines, have wings with drastically different inferred radial velocities, with values of -11 km s^{-1} and +10 km s^{-1} for the *h* and *k* lines, respectively. These results are still not understood and are difficult to interpret because of scattering effects and opacity broadening.

The new observational results for α Ori are a strong motivation to further explore acoustic shock wave models. It is therefore the goal of this paper to evaluate the formation of sub- and supersonic velocity patterns at different atmospheric heights. In particular, I will discuss monochromatic wave calculations having a fixed wave period and stochastic wave calcu-

lations with periods determined by a random number generator assuming modified Gaussian distributions. Understandably, the monochromatic wave models are not realistic and are only given as comparison. The paper is structured as follows: In Sect. 2, I discuss the method and model assumptions considered. Sect. 3 gives the results. Conclusions are presented in Sect. 4.

2. Method and model assumptions

I use an Eulerian one-dimensional, spherically symmetric, time-dependent radiation hydrodynamic code based upon the method of characteristics (Cuntz & Ulmschneider 1988). The code is suitable to study the propagation of shocks, which are treated as discontinuities. Boundary conditions for incoming and outgoing shocks are solved. Ionization of hydrogen is explicitly taken into account assuming a 3-level atom. It has been considered in a fully consistent manner both in the equations of thermodynamics and hydrodynamics. Noninstantaneous effects of hydrogen ionization have been omitted. The Lyman-α transition is computed by using first order escape probabilities as described by Hartmann & Avrett (1984). At the outer boundary of the atmosphere, the Lyman-α optical depth is assumed as $1 \cdot 10^8$ motivated by the Hartmann & Avrett model. Radiation damping is considered in the effectively thin plasma approximation based on a Cox and Tucker type law as given by Judge & Neff (1990). Judge (1990) presented theoretical arguments that the effectively thin plasma approximation should work well for chromospheric layers of the inactive, low-gravity star studied here.

I assume the following stellar parameters: $T_{\rm eff}$ = 3750 K, R_* = 800 $R_\odot$, and log g_* = 0.0 (cgs), which are the same as used by Basri et al. (1981). The Balmer continuum brightness temperature is assumed as $T_{\rm BC} = 0.8 \cdot T_{\rm eff}$. The initial atmosphere of the model extends up to 1.15 R_*, which corresponds to about 16 pressure scale heights in the hydrodynamic models. The atmospheric extent has been chosen to encompass the scale length where the major part of the mechanical energy dissipation of the shocks occurs. For my study I calculate the propagation of shock waves with an initial wave amplitude of 0.273 Mach corresponding to an energy flux of $1.6 \cdot 10^5$ ergs cm^{-2} s^{-1}. This wave energy flux is commensurate with measurements of chromospheric emission losses (Judge & Stencel 1991), which are believed to be directly related to the mechanical energy input. The shocks at a mass column density of log m = 1.08 (cgs), which corresponds to a position in the middle photosphere. The initial atmosphere is assumed to be isothermal with T = 2800 K. The reason for choosing shock waves over sinusoidal waves at the inner atmospheric boundary is due to findings of de Jager et al. (1991), who argued in favor of shock waves while trying to constrain photospheric motion fields of super- and hypergiant stars considering microturbulence data and wave travel restrictions.

Regarding the wave periods of the models, the following considerations need to be taken into account: Bohn (1984) found that the maximum acoustic energy flux occurs at the driving period $P_{\rm max} = \epsilon \cdot P_{\rm CO} = 4\pi c_z \epsilon / \gamma g_*$, where $P_{\rm CO}$ is the acoustic cutoff period, c_z is the sound speed at the top of the convection zone, γ is the ratio of the specific heats and g_* is the stellar surface gravity. Considering log g_* = 0.0 given above, $P_{\rm CO}$ can be estimated to $4.8 \cdot 10^6$ s. As the α Ori surface gravity is uncertain by at least a factor of 5, this value should not be considered reliable. In addition, the parameter ϵ, which denotes the position of the energy maximum in the acoustic frequency spectrum, is also largely unconstrained due to uncertainties in the calculation of the initial acoustic energy spectrum from the model of stellar convection (see e.g. Ulmschneider et al. 1996). These uncertainties are particularly relevant for stars of low gravity. Reasonable estimates of ϵ range from 0.2 to 0.5. Fortunately, the results for the acoustic shock wave models are not very sensitive to the shape of the frequency spectra anyhow, which reduces the relevance of above-mentioned uncertainties enormously.

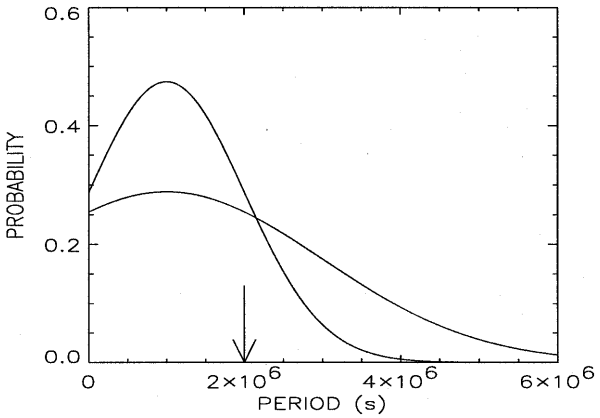

Fig. 1. Distribution functions for the wave periods of the narrow (Spectrum 1) and broad frequency spectrum (Spectrum 2) used as inner atmospheric boundary condition of the models. The wave period used in the monochromatic wave model is indicated by an arrow.

3. Results and discussion

3.1. Calculation of stochastic hydrodynamic models

For my study, I start with a monochromatic wave having a period of $1 \cdot 10^6$ s. In order to increase the stability of the hydrodynamic wave solutions, the radiation damping is switched on over a timespan of $5 \cdot 10^7$ s. The wave computation is continued over 3500 time steps, corresponding to $1.30 \cdot 10^8$ s. During that time 129 shocks are inserted into the atmosphere. The hydrodynamic atmosphere has then reached a dynamical steady state given by the balance of shock wave heating and radiative cooling.

Then I start to introduce shock waves with stochastically changing wave periods. I have selected two different wave period distributions. Both distributions are assumed to be Gaussian and centered at $1 \cdot 10^6$ s. The first distribution (Spectrum 1) has a standard deviation of $1 \cdot 10^6$ s, whereas the standard deviation of the second distribution (Spectrum 2) is $2 \cdot 10^6$ s (see Fig. 1). The spectrum has been cut off to avoid "negative periods." Periods below $1 \cdot 10^4$ s have also been excluded due to the limited hydrodynamic resolution in the wave models. The peak values

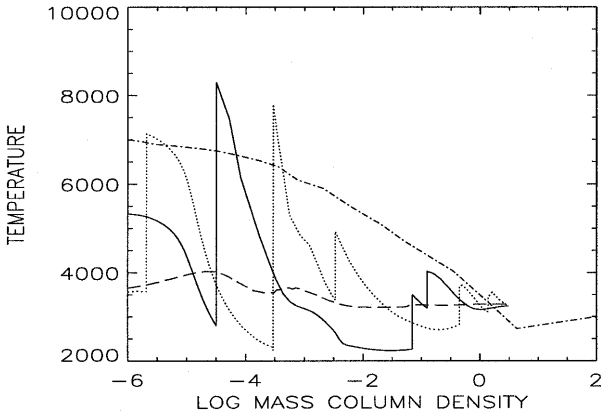

Fig. 2. Temperature distributions of two stochastic hydrodynamic models obtained $1.73 \cdot 10^7$ s and $1.82 \cdot 10^7$ s after acoustic frequency spectra have been employed (dotted and solid line, respectively). Also shown are the time-averaged temperature of the model (dashed line) and the temperature run of the semiempirical chromosphere model of Basri et al. (1981) (dashed-dotted line). The hydrodynamic model is calculated by using Spectrum 1.

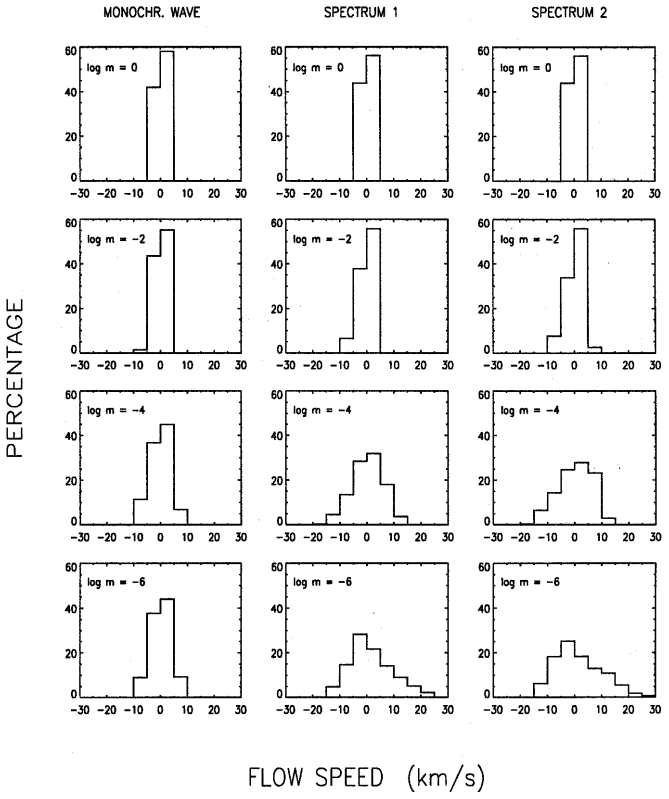

Fig. 3. Histograms for the flow velocities at different atmospheric heights indicated by the mass column density m (g cm^{-2}). Results are given for the monochromatic wave model and for Spectrum 1 and 2.

of the wave period distributions have been chosen according to results from traditional acoustic energy generation models (Bohn 1984; Ulmschneider et al. 1996). As comparison to these stochastic wave models, I also calculate a monochromatic wave model with $P = 2 \cdot 10^6$ s. Contrary to waves considering period distributions, monochromatic waves rely on a fixed wave period only. The above-given wave period has been selected to ensure that shock overtaking events are avoided, which are found to occur even in monochromatic wave computations with sufficiently small wave periods (Theurer et al. 1997).

Cuntz (1992a,b) already obtained some results concerning the behavior of stochastic wave models. He found that these models are characterized by shock-shock interaction due to the fact that a broad range of frequencies exists. The stochasticity of the wave field leads to episodic energy and momentum input to the atmosphere, which controls the temperature, the flow speed, and the thermodynamic quantities. The models are also characterized by a complicated hydrodynamic structure determined by a nonuniform distribution of shocks. The shock strengths and the shock speeds differ substantially and change non-monotonically with height. This result gives insight into the basic physics going on: after allowing the wave period to change stochastically, shocks with different strengths are introduced into the atmosphere. Different shock strengths cause different shock speeds leading to interacting, overtaking and merging of shocks ("shock-cannibalism"). Since the strength of an overtaking shock combines with the shocks it engulfs, its speed increases, so it overtakes more and more shocks in front of it and attains an even greater strength. Consequently, the amount of momentum and energy deposition that occurs varies drastically with time and atmospheric height. The direction of the flow alternates between outwardly and inwardly directed motions depending on the strengths of the shocks and the radiation-hydrodynamic history of the flow.

An example of that behavior is given in Fig. 2. It shows the temperature structure of a stochastic shock wave model at $1.73 \cdot 10^7$ s and $1.82 \cdot 10^7$ s after acoustic frequency spectra have been employed. It is found that the second and third shock (counted from lower to higher mass column densities) merge as the speed of the third shock is 11.5 km s^{-1} compared to 10.0 km s^{-1} of shock number two. Therefore, the post-shock temperature of the main shock increases from 7790 K to 8300 K while its strengths climbs from $M_{\rm sh} = 4.23$ to $M_{\rm sh} = 4.84$. The hydrogen ionization degree behind that shock also increases from 11.9% to 25%. The temperatures behind these shocks (which are extremely relevant for the formation of chromospheric line emission) clearly surpass those of the semiempirical chromosphere model of Basri et al. (1981), whereas the time-averaged atmospheric temperatures do not. They remain mostly between 3500 K and 4000 K, which is far beneath typical chromospheric values. This behavior is caused by quasi-adiabatic cooling preferably occurring in regions between the shocks. It is caused by the generation of considerable chromospheric velocity fields due to momentum transfer of strong shocks generated in the stochastic wave field.

3.2. Evaluation of chromospheric velocity fields

The main goal of this paper is to explore the consequences of shock-shock interaction for the generation of stochastic chromospheric velocity fields in α Ori in a systematic manner. Therefore, I evaluate the behavior of the flow at different atmospheric heights corresponding to distinct values of the mass column density m. My check points are: log m = 0, -2, -4, -6 (cgs). By performing sufficiently long computer runs, I calculate the likelihood for the flow of being subsonic, supersonic, inflowing or outflowing. I will discuss the probability distribution for the flow velocity by using increments of 5 km s^{-1}.

First of all, I evaluate the results for Spectrum 1. In order to minimize the impact of the starting model, which is the monochromatic wave model obtained at time step IT = 3500, I ignore the following $7 \cdot 10^6$ s for the statistical analysis. The wave computation is then continued over a timespan of $7.15 \cdot 10^7$ s. During that period of time, 51 shocks are inserted into the atmosphere. Due to overtaking and merging of shocks, strong atmospheric inflows and outflows are initiated. It is found that at relatively low mass column densities (i.e., farther out in the atmosphere) the likelihood for larger inflows and outflows increases (see Fig. 3). At log m = 0, the velocity of the flow stays within $\pm$5 km s^{-1} range. At log m = -2, the distribution is slightly broader, but does not exceed $\pm$10 km s^{-1}. At log m = -4 and -6, however, the likelihood for the flow being larger than +10 km s^{-1} or smaller than -10 km s^{-1} is 8% and 21%, respectively. On the other hand, the absolute value of the flow speed barely exceeds 15 km s^{-1}, except at log m = -6.

In the case of Spectrum 2, the results obtained are quite similar. It is found again that at log m = 0, the velocity of the flow velocity stays within $\pm$5 km s^{-1}. At log m = -2, the velocity distribution is again somewhat broader, but again does not exceed $\pm$10 km s^{-1}. At log m = -4 and -6, the likelihood for the absolute value of the flow for being larger than 10 km s^{-1} is now found to be 10% and 24%, respectively. The differences between Spectrum 1 and Spectrum 2 are insignificant, considering a margin of error of 2 percentage points. Huge differences however exist regarding the monochromatic wave calculation with $P = 2 \cdot 10^6$ s (see Fig. 3). I evaluated the behavior of the flow considering 20 wave periods. I found that the flow velocities almost never exceed the $\pm$5 km s^{-1} range at log m = 0 and -2 and never ever exceed the $\pm$10 km s^{-1} range. This result shows that acoustic frequency spectra are pivotal for generating chromospheric flow speeds outside the $\pm$10 km s^{-1} range, which have been suggested by observations (Carpenter & Robinson 1997).

Now I investigate the flow velocity u in comparison with the local sound speed c, which is given by the local atmospheric temperature and the hydrogen ionization degree. The fraction u/c (= Mach number) is a further important characteristic of the atmospheric flow field. The Mach number of the flow is again evaluated at distinct values of the mass column density in the hydrodynamic models by using increments of 0.5. In case of an inflow, u/c is negative, in case of an outflow u/c is positive. The absolute value of u/c then decides whether the flow is subsonic or supersonic. The models show the following results: In case of the monochromatic wave model with $P = 2 \cdot 10^6$ s, the flow is essentially subsonic in the entire atmospheric domain. The likelihood for the flow to become supersonic increases slightly from 0% at log m = 0 to 5% at log m = -6. In case of the Spectrum 1, however, the likelihood for the flow for being supersonic increases continuously with decreasing mass column density. At log m = -2, -4, and -6, the likelihood for supersonic flows is 7%, 28%, and 43%, respectively. The margin of errors in this numbers is again about 2 percentage point indicating that the trend is real. In case of Spectrum 2, the likelihood for supersonic flows also increases with decreasing mass column density with the numbers now being higher than for Spectrum 1. At log m = -2, -4, and -6 the likelihood is now 10%, 35%, and 52%, respectively. It shows that at low mass column densities (i.e., relatively far outward in the chromosphere), the atmospheric flow is very often supersonic when acoustic frequency spectra are adopted. The differences concerning the Mach numbers between the two spectra appear to be significant. The fact that dependencies on the employed spectra occur for the Mach numbers, but not for velocities itself, is caused by the discrepancies in the chromospheric temperatures. Spectrum 2 contains a higher number of long-period shock waves leading to significantly stronger shocks in the atmosphere. These shocks initiate additional momentum transfer and quasi-adiabatic cooling, which counteracts chromospheric heating.

4. Conclusions

I have presented new calculations for the generation of sub- and supersonic inflows and outflows in the chromosphere of α Ori (M2 Iab) as a consequence of stochastic energy deposition by acoustic shocks. These models are motivated by observational results from HST-GHRS which give information about the chromospheric dynamics in this star. I found the following results:

1. In case of stochastic shock waves the mechanical energy and momentum input to the atmosphere occurs episodically and is overwhelmingly controlled by strong shocks generated by shock merging. These shocks are thus responsible for generating stochastic chromospheric velocity fields.

2. In case of stochastic shocks, a relatively broad range of chromospheric velocities is encountered, which increases with decreasing mass column density. In the middle and outer chromosphere, the characteristic velocity range encompasses $\pm$10 and $\pm$15 km s^{-1}, depending on the height.

3. The difference between the chromospheric velocity distributions for the two inserted spectra appear to be insignificant. A much narrower velocity distribution however is found in case of the monochromatic wave model considered.

4. The range of velocities found in the stochastic wave computations appear to be consistent with the velocity intervals revealed by the Fe II emission line components observed by HST-GHRS, which are considered an important diagnostic tool for chromospheric dynamics of α Ori (Carpenter & Robinson 1997). De-

tailed studies of Fe II line formation are however needed to verify this picture.

5. Regarding the Mach numbers of the flow, it is found that supersonic inflows and outflows are easily produced by the stochastic wave models, contrary to the monochromatic wave model calculated. This result is in agreement with earlier results given by Cuntz (1992a,b).

6. In case that noninstantaneous ionization of hydrogen is considered, some of the results are expected to change, notably the u/c ratios. It is found that noninstantaneous hydrogen ionization tends to produce larger temperatures behind shocks (Carlsson & Stein 1991, 1992), while leaving the local velocity fields largely unaffected.

This work is part of ongoing efforts to understand outer atmospheric heating in stars of different spectral type and evolutionary status. In case of α Ori, it has previously been argued that the outer atmospheric structure might be attributable to the propagation of Alfvén waves (Hartmann & Avrett 1984). The problem however is that the models calculated so far are solely based on the adoption of a time-*independent* dissipation law for the wave energy flux in combination with the WKB approximation. Nevertheless, it should be noted that it is indeed possible that stochastic α Ori velocity fields may be associated with magnetic heating – a conjecture which still needs to be explored while considering time-dependent stochastic effects. Recent studies of non-WKB waves by Charbonneau & MacGregor (1995) which also consider Alfvén wave dissipation are not applicable to α Ori, as these models assume an isothermal atmosphere with $T \geq 30,000$ K. In order to ultimately verify the significance of acoustic waves for the outer atmosphere and wind of this star, detailed comparison of synthetic line spectra with observations have to be performed. Studies focussing on that issue are planned in the future.

Acknowledgements. I am pleased to acknowledge support for this work through the NASA Astrophysical Theory Program NAG 5-3027 and the HST Cycle 6 Archive Research Grant AR-06369.01-95A to the University of Alabama in Huntsville.

References

Basri G.S., Linsky J.L., Eriksson K., 1981, ApJ, 251, 162
Bohn H.U., 1984, A&A, 136, 338
Brandt J.C., et al., 1995, AJ, 109, 2706
Carlsson M., Stein R.F., 1991. In: Ulmschneider P., Priest E.R., Rosner R. (eds.) Mechanisms of Chromospheric and Coronal Heating, Springer, Berlin, p. 366
Carlsson M., Stein R.F., 1992, ApJ, 397, L59
Carpenter K.G., Robinson R.D., 1997, ApJ, 479, 970
Carpenter K.G., Robinson R.D., Wahlgren G.M., Linsky J.L., Brown A., 1994a, ApJ, 428, 329
Carpenter K.G., Robinson R.D., Judge P.G., Ebbets D.C., Brandt J.C., 1994b. In: Caillault J.-P. (ed.) Cool Stars, Stellar Systems, and the Sun VIII. ASP Conf. Series 64, San Francisco, p. 56
Charbonneau P., MacGregor, K.B., 1995, ApJ, 454, 901
Cuntz M., 1992a. In: de Jager C., Nieuwenhuijzen H. (eds.) Instabilities in Evolved Super- and Hypergiants, North Holland Publishers, Amsterdam, p. 133
Cuntz M., 1992b. In: Giampapa M.S., Bookbinder J.A. (eds.) Cool Stars, Stellar Systems, and the Sun VII. ASP Conf. Series 26, San Francisco, p. 383
Cuntz M., Ulmschneider P., 1988, A&A, 193, 119
de Jager C., de Koter A., Carpay J., Nieuwenhuijzen H., 1991, A&A, 244, 131
Hartmann L., Avrett E.H., 1984, ApJ, 284, 238
Judge P.G., 1990, ApJ, 348, 279
Judge P.G., Neff D.H., 1990. In: Wallerstein G. (ed.) Cool Stars, Stellar Systems, and the Sun VI. ASP Conf. Series 9, San Francisco, p. 57
Judge P.G., Stencel R.E., 1991, ApJ, 371, 357
Newell R.T., Hjellming R.M., 1982, ApJ, 263, L85
Robinson R.D., Carpenter K.G., 1995, ApJ, 442, 328
Theurer J., Ulmschneider P., Cuntz M., 1997, A&A (in press)
Ulmschneider P., Theurer J., Musielak Z.E., 1996, A&A, 315, 212

This article was processed by the author using Springer-Verlag LaTeX A&A style file *L-AA* version 3.